Title

Optimization of Campesterol-Producing Yeast Strains as a Feasible Platform for the Functional Reconstitution of Plant Membrane-Bound Enzymes

Journal

ACS Synthetic Biology, 12(4)

ISSN

2161-5063

Authors

Xu, Shanhui

Teng, Xiaoxuan

Li, Yanran

Publication Date

2023-04-21

DOI

10.1021/acssynbio.2c00599

Peer reviewed

HHS Public Access

Author manuscript

ACS Synth Biol. Author manuscript; available in PMC 2024 November 03.

Published in final edited form as:

ACS Synth Biol. 2023 April 21; 12(4): 1109–1118. doi:10.1021/acssynbio.2c00599.

Optimization of Campesterol-Producing Yeast Strains as A Feasible Platform For the Functional Reconstitution of Plant Membrane-Bound Enzymes

Shanhui Xu[1], **Xiaoxuan Teng**[1], **Yanran Li**[1,*]

[1]Department of Chemical and Environmental Engineering, University of California, 900 University Avenue, Bourns Hall, Suite A220, Riverside, California 92521, USA

Abstract

Campesterol is a major phytosterol that plays important roles in regulating membrane properties and serves as the precursor to multiple specialized metabolites such as the phytohormone brassinosteroids. Recently, we established a campesterol-producing yeast strain and extended the bioproduction to 22-hydroxycampesterol and 22-hydroxycampest-4-en-3-one, precursors to brassinolide. However, there is a tradeoff in growth due to the disrupted sterol metabolism. In this study, we enhanced the growth of the campesterol-producing yeast by partially restoring the activity of the sterol acyl transferase and engineering upstream FPP supply. Furthermore, genome sequencing analysis also revealed a pool of genes possibly associated with the altered sterol metabolism. Retro engineering implies an essential role of ASG1, especially the C-terminal asparagine-rich domain of ASG1, in the sterol metabolism of yeast especially under stress. The performance of the campesterol-producing yeast strain was enhanced with the titer of campesterol to 18.4 mg/L, and the stationary OD_{600} was improved by ~ 33% comparing to the unoptimized strain. In addition, we examined the activity of a plant cytochrome P450 in the engineered strain, which exhibits more than 9-fold higher activity than when expressed in the wild-type yeast strain. Therefore, the engineered campesterol-producing yeast strain also serves as a robust host for the functional expression of plant membrane protein.

Keywords

campesterol; yeast; metabolic engineering; genome-scale screening; membrane-bound enzymes

Introduction

Sterols are essential membrane components in mammals, plants, fungi, and bacteria, regulating membrane fluidity and permeability[1], and involved in protein trafficking and signal transduction[2]. Different organisms produce different types of sterols. Mammals produce cholesterol that serves as the precursor to steroid hormones, bile acids, and

*Correspondence should be addressed to Yanran Li, FAX: 951.827.3188, yanranl@ucr.edu.

Author contributions

S.X. and Y.L. conceived of the project, S.X., X.T., and Y.L. designed the experiments, analyzed the results, and wrote the manuscript.

Competing financial interests: The authors declare that there is no conflict of interest regarding the publication of this article.

vitamin D; fungi produce ergosterol, the precursor of vitamin D2; plants produce a mixture with campesterol and β-sitosterol as the dominant components[1]. Phytosterols function as precursors to several plant specialized metabolites, such as the plant hormone brassinosteroids (BRs) and the pharmaceutically intriguing withanolides. Similar to sterol hormones in animals, BRs play important roles in regulating plant growth and development, as well as resistance to biotic and abiotic stress[3].

Cholesterol has been reported to modulates the function of various types of membrane proteins[4], such as receptors, ion channels, transporters, and peptides, either by directly binding to the proteins or indirectly affecting membrane properties. The cholesterol-producing yeast has been believed to provide a more preferred membrane microenvironment for the functional reconstitution of mammalian membrane proteins, and has been validated by enhanced stability and activity of a Na,K-ATPase α3β1 isoform in a "humanized" cholesterol-producing *Pichia pastoris* strain[5]. Similarly, the composition of the plasma membrane has been shown to be critical to the activity of membrane proteins in plants[6]. Phytosterols differ from cholesterol and ergosterol primarily in the side chains, e.g., campesterol and sitosterol are equipped with a C24-methyl or C24-ethyl group, respectively. Plants exhibit distinct membrane properties from fungi and metazoans, such as lower membrane ordering than cholesterol or ergosterol composed membrane[1]. Plant membrane proteins play important roles in plant perception, immunity, and metabolism[7, 8]. The microenvironment created by phytosterols is believed to be crucial for optimal enzymatic activities[9]. Thus, a phytosterol-producing yeast strain might also function like a "plantinized" yeast more adapted to the functional reconstitution of plant membrane proteins. However, whether phytosterol-producing yeast exhibits similar characteristics remains to be explored.

In our previous study, we engineered *Saccharomyces cerevisiae* to produce campesterol instead of ergosterol and reconstituted the early-stage pathway towards the synthesis of BRs[10]. The biosynthesis of campesterol was achieved using plant enzymes DWF1, DWF5, and DWF7 in *S. cerevisiae* (Figure 1). Further upregulation of upstream mevalonate (MVA) pathway enzymes enhanced the production of campesterol yet not accessible to downstream biosynthetic enzymes, and further investigation implies that it is mainly because phytosterols are almost completely esterified in the engineered strain. Thus, acyltransferases ARE1, ARE2, and sterol C-24(28) reductase ERG4 were inactivated to yield yeast strain YYL65 to produce free campesterol that is accessible to the downstream enzyme such as CYP90B1. However, YYL65 exhibits significant growth burden due to these genetic modifications. The growth rate at the exponential phase of YYL65 decreased to 1/7 of the wild-type. The OD_{600} at the stationary phase of YYL65 was reduced to less than 1/2 of that of the wild-type yeast strain under the same cultivation condition. Further adaptive evolution of YYL65 generated YYL67 with both enhanced growth (stationary OD_{600} only ~ 2/3 of wild-type) and campesterol production (7 mg/L), yet YYL67 still grows much weaker than the wild-type yeast. Additionally, YYL67 has lower tolerance to Li^+ and heat, compared to the wild-type.

In this study, we extended the engineering efforts to further enhance the performance of the engineered phytosterol-producing yeast platform. In addition to more robust growth,

the engineered strain also exhibits higher resistance to Li^+ and heat. We also examined whether the change of the sterol composition could plantinize the engineered yeast strain through testing the activity of a cytochrome P450 CYP82Y1 in the optimized campesterol-producing yeast strains. Surprisingly, the activity of CYP82Y1 in producing 1-hydroxy-N-methylcandadine was enhanced by more than 9-fold in the engineered campesterol-producing strains than that in the wild-type yeast strain. The engineered yeast strain not only serves as a more robust platform to produce campesterol, further reconstitute and investigate BR biosynthesis, but also as a potential workhorse for the functional reconstitution of plant membrane-bound proteins.

Results and Discussion

Partially restoring the function of acyltransferases can rescue yeast growth

Previously, the inactivation of the two acyl-CoA sterol acyltransferases ARE1 and ARE2 in YYL67 (Table S1) resulted in the synthesis of free campesterol as well as an evident growth deficiency[10]. The growth deficiency is likely caused by the defected sterol biosynthesis as well as the potential toxicity of free phytosterols, specifically campesterol in yeast. Prior investigation showed that ARE1 and ARE2 exhibit distinct substrate specificity: ARE2 prefers ergosterol as the substrate while ARE1 has higher promiscuity and prefers sterol precursors than the end product ergosterol[11]. Thus, ARE1 and ARE2 were each introduced into YYL67 with different expression conditions (different promoter strengths and intracellular localization) to find a solution that can restore the growth of YYL67 with a minimal effect on campesterol production. ARE1 and ARE2 were expressed downstream of either a strong constitutive *PYK1* promoter (P_{PYK1}) or a weak *CYC1* promoter (P_{CYC1}), with the native promoter of *ARE2* (400bp upstream of *ARE2,* P_{native}) as a control. In addition, C-terminal signaling peptides were directly fused to the C-terminus of ARE1 and ARE2 to redirect the acyltransferases to localize on organelles besides the endoplasmic reticulum (ER) membrane, where ARE1 and ARE2 are natively localized and where sterols are synthesized and esterified[12]. Peroxisomes and Golgi apparatus are both phospholipid-bilayer single membrane organelles with similar membrane structures to ER, which is needed to support the correct folding of AREs. Thus, the effects of the following two signal peptides were examined: the C-terminal tag-SKL that was reported to localize enzymes to peroxisomes[13], and the C-terminal tag -KVD which was a Golgi retention C-terminal motif[14]. The localization of ARE1, ARE2 with C-terminus tags was confirmed in YYL63 (Δ*are1*Δ*are2*; Table S1) using confocal fluorescence microscopy (Figure S1). The C-terminus tag -SKL led ARE2 to peroxisomes which were marked by a native peroxisomal membrane protein PEX3-YFP[15]; the C-terminus tag -KVD led ARE2 to Golgi which was marked by a native Golgi membrane protein VRG4-Dsred[15] (Figure S1). The OD_{600} of each strain at stationary phase was measured as an indicator of yeast growth, and the productions of free and total (including free and esterified form) campesterol and the precursor 24-methylenecholesterol (the two major phytosterols synthesized in YYL67) were estimated (Figure 2). Free sterols were extracted using *Extraction Method A* (Materials and Methods) without saponification, while “total sterols” (both free sterols and sterol esters) were extracted using *Extraction Method B* (Materials and Methods). Due to the harsh saponification procedure involving high concentration treatment of KOH, using *Extraction*

Method B exhibits a lower efficiency compared to *Extraction Method A* in recovering the corresponding sterols.

As expected, introducing ARE1 or ARE2 into YYL67 generally resulted in enhanced stationary OD_{600}, and the production of free campesterol was decreased but at different levels. Notably, ARE1 and ARE2 exhibit distinct esterification efficiency towards campesterol and 24-methylenecholesterol. When expressed downstream of the constitutive P_{PYK1} in YYL67, ARE2 enhanced the level of total campesterol by ~7 folds with ~60% decrease of free campesterol, while expressing ARE1 downstream of P_{PYK1} did not change the level of total campesterol much in YYL67 but substantially decreased the level of free campesterol (Figure 2A). This set of data indicates that ARE2 more efficiently esterifies campesterol compared to ARE1. Meanwhile, the production of 24-methylenecholesterol was significantly enhanced when ARE1 or ARE2 was introduced into YYL67 and regulated by P_{PYK1} (Figure 2B). Notably, ARE2 expressed downstream of P_{native} in YYL67 showed lower production of free campesterol and campesterol ester, compared to when ARE2 was expressed downstream of P_{PYK1}, which is likely due to the lower strength of P_{native} of ARE2 than P_{PYK1}. Similar phenotypes (enhanced growth, enhanced production of 24-methylenecholsterol in ester form) were observed when ARE1 was expressed downstream of weak P_{CYC1} or redirected to other organelles than ER (Figure 2B). However, under the same expression conditions (downstream of P_{CYC1} or redirected to the other organelles than ER), ARE2 exhibits a similar phenotype to YYL67. This indicates that ARE1 is relatively more efficient in esterifying 24-methylenecholesterol than ARE2. Although ARE1 and ARE2 can both esterify campesterol and 24-methylenecholesterol when expressed at high level at ER membranes, they do exhibit distinct substrate specificity. The observation that ARE1 prefers 24-methylenecholesterol (unsaturated C24-28) is consistent with previous reports that ARE1 prefers yeast sterol intermediates with unsaturated C24-28[11]. ARE2, on the other hand, prefers campesterol (saturated C24-28) and ergosterol (saturated C24-28) as reported[11].

SAT1 is a plant sterol O-acyltransferase from *Arabidopsis thaliana* and was characterized to esterify mainly phytosterol precursors, such as cycloartenol and lanosterol, while campesterol is not its favorable substrate[16]. Thus, we also introduced SAT1 into YYL67, downstream of a strong P_{PYK1} to enhance the growth and minimize the effects on the production of free campesterol. Although SAT1 barely esterified 24-methylenecholesterol or campesterol, expressing SAT1 in YYL67 did enhance the stationary OD_{600} (Figure 2). Since SAT1 has been reported to mainly function at the upstream part of the sterol biosynthesis, the level of lanosterol was measured (Figure 2B). Consistent with previous investigations[16], a significant amount of lanosterol in the ester form was detected only when SAT1 was expressed in YYL67, which also exhibited a higher stationary OD_{600} than YYL67 alone. These results indicate that although sterol esters do not directly constitute membrane, they play a role in yeast growth under stress condition. In general, the growth of yeast strain seems to be positively correlated with the total levels of sterols (mostly in ester form), either lanosterol or phytosterols (Figure 2B). ARE2 expressed downstream of P_{PYK1} was selected for the subsequent study due to the relatively robust growth and higher free campesterol production among strains with higher stationary OD_{600} than YYL67.

Increasing production of FPP or GGPP can improve the growth of YYL67

ERG20 is a farnesyl pyrophosphate synthetase (FPS) that catalyzes the conversion of isopentenyl pyrophosphate (IPP) to geranyl pyrophosphate (GPP) and GPP to farnesyl pyrophosphate (FPP). FPP is the precursor to steroid synthesis and has often been engineered to enhance yeast growth or isoprenoid precursor supply[17, 18, 19] $ERG20^{F96C}$ has been identified to be a dual function enzyme that is not only able to synthesize FPP but also exhibits the function of BTS1, the native geranylgeranyl diphosphate synthase (GGPPS) in yeast, to convert FPP to geranylgeranyl diphosphate (GGPP) (Figure 1). Overexpressing $ERG20^{F96C}$ into yeast was reported to improve the production of diterpenes, and the improvement was higher than overexpressing BTS1[18]. In addition to $ERG20^{F96C}$, $ERG20^{A99G}$ was reported to improve the growth and increase the total isoprene production[19]. $ERG20^{F96C}$, $ERG20^{A99G}$, wild-type ERG20, and BTS1 were expressed downstream of a constitutive promoter P_{TEF1} in YYL67, all of which resulted in enhanced growth but decreased production of campesterol by ~22 folds, ~1.3 folds, 0.8 folds and ~4 folds, respectively (Figure 3A, 3B). No accumulation of 24-methylenecholesterol or lanosterol was detected. The enhanced growth when expressing $ERG20^{F96C}$ and BTS1 indicates that YYL67 is likely deficient in GGPP supply, while the decrease in campesterol production is likely due to the enhanced consumption of FPP towards GGPP by the function of $ERG20^{F96C}$ and BTS1 as GGPPS.

$ERG20^{A99G}$ exhibited the most enhanced growth as well as the least decreased campesterol production in comparison to YYL67 and was introduced into YYL67 along with *ARE2* through genome integration to generate YYL102 (Table S1) for downstream optimization. The optimized strain YYL102 has higher growth rate and a minor decrease of campesterol production compared to YYL67 (Figure 3C, 3D). A time-course on the production of free campesterol in YYL67 and YYL102 were also monitored. Interestingly, the production of free campesterol in YYL67 was peaked around 24 hours after inoculation and slightly decreased afterwards, while YYL102 exhibits a growing trend through the 72-hours of fermentation (Figure S2). The tolerance of YYL102 to Li^+ and heat was increased substantially as well (Figure 3E), which implies that YYL102 is more robust than YYL67. In addition, Li^+ and heat tolerance are two important parameters that affect the efficiency of yeast transformation, and YYL102 exhibits higher transformation efficiency than YYL67.

Genome sequencing of YYL67 provides candidates to engineer for further optimization of growth and campesterol production

YYL67 is an adaptive-evolved strain exhibiting higher production of campesterol and more robust growth in comparison to its parental strain, YYL65[10]. The mutations in YYL67 may play a role in enhancing the growth and campesterol production, and are also promising candidates to engineer for enhanced performance of the strain. Therefore, we sequenced the genomes of YYL65, YYL67, and another evolved strain YYL65-5[10]. Paired-end libraries (150-bp) were generated by NGS platforms and sequenced to an average depth of over 50× for each strain. The high coverage enabled reliable genome-wide analysis of insertion and deletion (InDel) and single-nucleotide polymorphisms (SNPs), which were widely found through the genomes of YYL67 and YYL65-5 (Figure S3, Table S1, S3, S4, S5). Compared to the parental strain YYL65, YYL67 and YYL65-5 carry 27 and 35 InDels in gene-coding

regions (Table S4), respectively. 18 of these InDels are present in both YYL67 and YYL65-5 (Table S4); many of these genes are related to transcriptional regulation and growth stress response (Table S3B). On the other hand, approximately 300 SNPs occur within open reading frames (ORFs) in YYL67 and YYL65-5. The SNPs affect 19 genes in YYL67 and 22 genes in YYL65-5 at amino acid level, with 14 genes found in both YYL67 and YYL65-5 (Table S3C and S5). The genes affected by InDels or SNPs were considered promising candidates to engineer for enhanced growth or campesterol production in yeast.

To examine the influence of these genes on the growth and sterol production in YYL67, the 41 mutated genes (27 from InDel analysis, 19 from SNPs, with 3 redundant genes with both InDels and SNPs, 2 genes cannot be inactivated due to technique problems, Table S4–S6) were inactivated individually in YYL67 as well as the wild-type CEN.PK2-1D using CRISPR/Cas9 system. Although the inactivation of most of the genes did not result in any change of phenotypes compared to the negative control (inactivation of the corresponding gene in CEN.PK2-1D, Figure S4), inactivation of ASG1 was lethal to YYL67 and greatly deteriorated the growth of wild-type yeast. Thus, ASG1 was considered an important gene contributing to YYL67's enhanced performance in comparison to the parental strain YYL65 (Figure S4). ASG1 is an activator of stress response genes and the null mutants of ASG1 have a respiratory deficiency. We quantified the mRNA level of ASG1 in YYL67, the parental strain YYL65, and the growth optimized strain YYL102 by reverse transcription polymerase chain reaction (RT-PCR). The transcription level of ASG1 was the highest in YYL65, the one with the lowest growth rate[10] among the three strains (Figure S5). Meanwhile YYL102 had the most robust growth among the three strains exhibited the lowest level of *ASG1* mRNA (Figure S5). This result suggests that ASG1 is likely to be overexpressed when the strain is under stress.

ASG1 was then upregulated in YYL67 by introducing an extra copy of the genes for further analysis. *ASG1* gene was cloned from genomic DNA of YYL67 (marked as $ASG1^{m}$) and YYL65 (marked as $ASG1^{ori}$). The cloned genes were sequenced, and $ASG1^{m}$ has one less asparagine (N) at the C-terminal N-rich region, compared to $ASG1^{ori}$ (Table S2, S7). Both versions of ASG1 were expressed downstream of the strong, constitutive *GPD* promoter (P_{GPD}) from a low-copy number plasmid in YYL67 and YYL102 (Table S2). Surprisingly, the overexpression of ASG1 in YYL67 enhanced the campesterol production by ~ 1 fold but did not improve the yeast growth (Figure 4A). However, the overexpression of ASG1s in the more robust strain YYL102 did not lead to significant change in either the stationary OD_{600}, the free campesterol production (Figure 4A), or the saponified total campesterol level (Figure S6A). ASG1 likely plays a role in sterol metabolism in yeast under stress condition. In addition, overexpression of $ASG1^{ori}$ in YYL67 enhanced campesterol production to a slightly higher extent than overexpression of $ASG1^{m}$, which hints at the importance of the N-rich region to the function of ASG1. $ASG1^{\Delta N}$ without N-rich region and $ASG1^{½N}$ with half of the N-rich region were constructed and overexpressed downstream of P_{GPD} in YYL67 and YYL102 (Table S2, S7, Figure 4A). In YYL67, $ASG1^{\Delta N}$ resulted in the highest production of campesterol (~2-fold higher) among all the mutants with a similar stationary OD_{600} in comparison to YYL67, and $ASG1^{½N}$ showed similar phenotype as $ASG1^{m}$. No significant differences in campesterol production, either in free or esterified form, were detected when overexpressing ASG1 and mutants in YYL102 (Figure 4A, S6A).

To investigate how ASG1 responds to the growth stress, YYL67 expressing different ASG1 variants or mutants were cultured in two different medium conditions: synthetic defined medium (SDM) supplemented with 5% ethanol and 2×SDM supplemented with 4% glucose, representing culture conditions under stress[20] and with extra nutrients, respectively. When cultured in 2× SDM, YYL67 expressing ASG1 and mutants exhibit more robust growth and a similar level of campesterol production, compared to when cultured in the standard medium (Figure 4B). On the other hand, in the presence of 5% ethanol, the expression of $ASG1^{ori}$ or $ASG1^{m}$ did not result in obvious changes in yeast growth or campesterol production in comparison to YYL67 harboring an empty vector (negative control, NC); while the introduction of $ASG1^{\Delta N}$ or $ASG1^{½N}$ into YYL67 decreased both the growth and the campesterol production comparing with NC (Figure 4C). Interestingly, the stationary OD_{600} was positively correlated with the length of the N-rich region of ASG1 when cultured in the presence of 5% ethanol: YYL67 expressing $ASG1^{\Delta N}$ showed the lowest OD_{600} ~5.0, while $ASG1^{ori}$ did not affect the growth of YYL67 much (Figure 4C). The different influences of expressing $ASG1^{\Delta N}$ and $ASG1^{ori}$ under stress (5% ethanol) suggests that the N-rich region of ASG1 plays an important role in the stress response in yeast, which is related to yeast growth and the sterol synthesis. As the N-rich region is usually related to protein aggregation[21], the morphology of $ASG1^{\Delta N}$, $ASG1^{½N}$, and $ASG1^{ori}$ was examined by confocal fluorescence microscopy (Figure S7). However, the deletion of N-rich region did not affect the aggregation morphology of ASG1 in yeast. This agrees with the previous study on another yeast transcription factor AZF1 that the deletion of N-rich region does not affect the localization or prion formation[22]. Further mechanistic investigations are needed to understand the precise role of ASG1 and the function of its N-rich region in yeast metabolism and stress response.

Among the other genes that were inactivated in YYL67, *IMD2* also significantly deteriorated the growth of YYL67 but was not lethal, yet did not affect the growth of CEN.PK2-1D (Figure S4). IMD2 is inosine monophosphate dehydrogenase, catalyzing the rate-limiting step in GTP biosynthesis[23]. IMD2 was then cloned from the genomic DNA of YYL67 (marked as $IMD2^{m}$) and YYL65 (marked as $IMD2^{ori}$). $IMD2^{m}$ has 7 mutated sites at amino acid level than $IMD2^{ori}$ (Table S7). $IMD2^{m}$ and $IMD2^{ori}$ were individually overexpressed in YYL67 and YYL102 downstream of the P_{GPD} from a low-copy number plasmid, but no significant effects on the growth or campesterol production were observed (Figure 4D). This result suggests that IMD2, though nonessential, plays a role in yeast growth, but not specifically involved in sterol metabolism or stress. Similarly, the inactivation of *FIG2* was lethal to YYL67 and severely deteriorated the growth of wild-type yeast (Figure S4). FIG2 has been found to involve in cell wall adhesin and is expressed during mating[24]. *FIG2* from YYL67 and the parental strain YYL65 were then cloned from genome DNA and sequenced, yet the sequencing results showed no mutations in *FIG2* of YYL67 compared to the wild-type yeast. The inconsistency is likely due to poor alignment of the corresponding contigs containing repetitive regions of the genes. Overexpression of FIG2 in YYL67 and YYL102 downstream of P_{GPD} from a low-copy number plasmid showed no significant effects on the growth or campesterol production (Figure S6B).

In this genome-scale screening, we found an interesting protein ASG1, which is involved in yeast stress regulation and the upregulation of ASG1 enhanced the production of

campesterol in YYL67. Nevertheless, the improvement of the strain performance during the adaptive evolution is likely due to the synergistic effect of multiple-gene mutations, instead of a single gene *ASG1* mutation. In addition, due to the lack of open-source genome information of CEN.PK2-1D and the limited number of biological replicates sequenced, the InDels and SNPs proposed from the genome analysis did not describe the genetic divergences between YYL67 (built from CEN.PK2-1D) and its parental strain YYL65 precisely enough. For future study, more systematic analysis, such as Genome-wide association studies (GWAS) analysis using the genome sequencing data of more biological replicates, coupled with systematic metabolite analysis will enable us to thoroughly understand the mechanism of yeast to adapt the growth and metabolic burden caused by altered genetic material and sterol metabolism.

The presence of free campesterol enhanced the activity of plant membrane enzyme In yeast

Membrane composition and morphology are essential for the activities of plant membrane proteins, which are heavily involved in plant metabolism and defense[7]. The altered sterol composition in the yeast strains may provide a different microenvironment for the functional reconstitution of plant membrane proteins. We examined the activity of a cytochrome P450 CYP82Y1, which converts N-methylcanadine to 1-hydroxy-N-methylcanadine, in the set of phytosterol-producing strains we constructed in this study: YYL56 (producing campesterol ester)[10], YYL64 (producing free 24-epicampesterol at the titer of 5.7 mg/L, the stereoisomer of campesterol due to the presence of *ERG4* in yeast)[10], YYL67 (producing free campesterol at the titer of 7.1 mg/L), and YYL102 (producing free campesterol with enhanced growth at the titer of 5.4 mg/L) (Table S1). CYP82Y1 was expressed downstream of a constitutive promoter *TPI1* (P_{TPI1}) from a low copy number plasmid (Table S2). TNMT was co-expressed with CYP82Y1 to afford the synthesis of the precursor of CYP82Y1, N-methylcanadine (Figure 5). Yeast strains were cultured in SDM medium fed with 12.5 μM canadine, the substrate of TNMT. The activity of CYP82Y1 was estimated using the production of 1-hydroxy-N-methylcanadine, the product of CYP82Y1. CYP82Y1 exhibited similar level of activities in YYL56 (Table S2), the strain producing campesterol mainly in the easter form, and the wild-type yeast strain (CEN-PK2.1D). Surprisingly, in comparison to CEN-PK2.1D, the production of 1-hydroxy-N-methylcanadine was up to 3-fold higher in YYL67, ~ 4-fold higher in YYL102, but only ~1-fold higher in YYL64 (Figure 5). On the other hand, the enzymatic activity of TNMT1, likely a cytosolic enzyme, exhibited the same efficiency towards the synthesis of N-methylcanadine across different campesterol-producing yeast strains (Figure S8A). Our results indicate that the presence of free campesterol in yeast does “plantinize” the yeast membranes (both plasma membranes and intracellular membranes) and enhance the enzymatic efficiency of plant membrane-bound proteins.

Furthermore, we examined the activity of another group of membrane-bound enzymes, steroid 5α-reductases converting progesterone to 5α-dihydroprogesterone, from both plants and mammals: *At*DET2 from *A. thaliana* and *Hs*SRD2 from *Homo sapiens* in the wild-type yeast strain and YYL67 (Figure S9). Each 5α-reductase was expressed downstream of P_{GPD} through a low-copy number plasmid. 300 μM of progesterone was fed to the yeast

culture and its reduced product 5α-dihydroprogesterone was examined. *At*DET2 exhibited enhanced production of 5α-dihydroprogesterone in YYL67 compared to the wild-type yeast strain, while *Hs*SRD2 showed no difference in the production of 5α-dihydroprogesterone in different strains (Figure S9). These results further implies that the enhanced activity of CYP82Y1 or *At*DET2 in YYL67 is very likely due to the presence of free campesterol, which may provide a more favorable microenvironment for the functional reconstitution of plant membrane bound proteins.

Because it was found that overexpressing $ASG1^{\Delta N}$ in YYL67 enhanced the production of free campesterol, we wished to investigate the effect of free campesterol level on the activity of CYP82Y1 in yeast, so $ASG1^{\Delta N}$ was co-expressed with TNMT1 and CYP82Y1 in YYL67. Interestingly, co-expressing $ASG1^{\Delta N}$ did not enhance the enzymatic efficiency of CYP82Y1 in YYL67 although the titer of free campesterol was ~2-fold higher than that of YYL67 (Figure 5, S8B). On the other hand, co-expressing $ASG1^{\Delta N}$ enhanced the enzymatic efficiency of CYP82Y1 in YYL102 although the titer of free campesterol is the same in comparison with YYL102 alone (Figure 5, S8B). Although free campesterol is an essential component for the “platinization” of the yeast membrane, the activity of plant membrane enzyme is not positively correlated with the amount of free sterol.

We also observed enhancement in the activity of CYP82Y1 in both YYL67 and YYL102 expressing $ASG1^{\Delta N}$ when cultured in the 2× SDM (in comparison to the standard SDM; Figure 5). Since culturing in 2× SDM did not enhance the level of campesterol in either YYL67 or YYL102 (Figure S8B) expressing $ASG1^{\Delta N}$ in comparison to standard SDM, this further implies that the activity of plant membrane-bound enzymes is not positively correlated with the level of free phytosterol in yeast. However, how $ASG1^{\Delta N}$ improves the functional reconstitution of CYP82Y1 in YYL102 but not YYL67 remains unclear.

In this study, we further optimize the “plantinized” yeast platform by partially restoring sterol esterification mechanism, engineering upstream FPP pathway, and performing retro genetic engineering. The enhanced growth, Li^+ and heat tolerance ensures the applications of this platform to reconstitute plant membrane anchored enzymes. The discovery of ASG1’s roles in yeast growth and sterol production under stress as well as plant membrane-bound enzyme reconstitution highlights ASG1 as an important target for further investigation and engineering for sterol-related metabolic engineering in yeast. The potential bottleneck to further enhance the production of campesterol and the growth of the strain is likely correlated with the endogenous sterol metabolism regulations, which functions to keep the equilibrium between free sterols and sterol esters and thus prevent an excessive free campesterol production. In addition, the massive accumulation of 24-methylenecholesterol when AREs were overexpressed indicates that the conversion of 24-methylencholesterol from campesterol catalyzed by DWF1 is also likely one of the key rate-limit steps. Thus, enhancing the enzymatic efficiency of DWF1 should also be investigated to further enhance campesterol production.

Materials and Methods

Materials

Campesterol (~98%) was obtained from Sigma-Aldrich. Yeast strains were cultured at 30 °C in complex yeast extract peptone dextrose (YPD, all components from BD Diagnostics) medium or synthetic defined medium (SDM) containing yeast nitrogen base (YNB) (BD Diagnostics), ammonium sulfate (Fisher Scientific), 2% (w/v) glucose unless specified and the appropriate dropout (Takara Bio) solution for selection.

General technique for DNA manipulation

PCR reactions were performed with Expand high Fidelity system (Sigma-Aldrich), Phusion DNA Polymerase (NEB), Q5 High-Fidelity DNA Polymerase (New England Biolabs) or Taq Polymerase (NEB) according to manufacturer's protocols. PCR products were purified by Zymoclean Gel DNA Recovery Kit (Zymo Research). Plasmids were prepared with Econospin columns (Epoch Life Science) according to manufacturer's protocols. All DNA constructs were confirmed through DNA sequencing by Azenta life science Inc. BP Clonase II Enzyme Mix, Gateway pDONR221 Vector, LR Clonase II Enzyme Mix (Life Technologies), and the *S. cerevisiae* Advanced Gateway Destination Vector Kit [25] (Addgene) were used to perform the Gateway Cloning. The Gibson one-pot, isothermal DNA assembly[57] was conducted at the scale of 10 μL by incubating T5 exonuclease (NEB), Phusion polymerase (NEB), Taq ligase (NEB) and 50 ng of each DNA fragment at 50 °C for 1 hour to assemble multiple DNA fragments. Yeast strains are constructed through homologous recombination and DNA assembly[58]. Yeast strains, plasmids, and sequences of genes used in this work are listed in Table S1, Table S2, and Table S7, respectively.

Culture conditions

For metabolite analysis, yeast strains were first cultured overnight in 500 μL SDM with 2% (w/v) glucose in 96-well plates (BD faulcon) at 30 °C overnight, at 250 r.p.m.. Appropriate volume of the overnight seed culture was inoculated in fresh 500 μL SDM with glucose to make OD_{600} around 0.1 and incubated at 30 °C for 72 hours before metabolite analysis of the yeast pellets. To monitor the growth, yeast strains were grown in 2 mL SDM with 2% (w/v) glucose in test tubes. The yeast strains were first cultured overnight in 500 μL SDM with 2% (w/v) glucose. Appropriate volume of the overnight culture was inoculated in fresh 2 mL SDM with 2% (w/v) glucose to make OD_{600} around 0.1 and incubated at 30 °C for 72 hour, at 250 r.p.m.. Yeast growth was monitored through measuring OD_{600}: appropriate amount of yeast culture was collected into the cuvette and diluted with water as needed to make the reading within the linear range of the instrument (usually from OD_{600} 0.1 to 0.8). OD_{600} of the culture was measured by Nanodrop (Molecular Device™).

For the cultivation in SDM supplemented with 5% ethanol, 2% (w/v) glucose was used as carbon source, and 5% (v/v) ethanol was added as the stress inducer. The 2×SDM medium contains 4% of glucose, 2× concentration of dropout, 2× concentration of nitrate bases and 2× concentration of ammonium sulfate.

Analysis and quantification of phytosterols in yeast

Phytosterols were collected and analyzed from yeast pellets. *Extraction Method A:* To extract free sterols from yeast, 100 μL acetone was added to yeast cell pellets (from 500 μL yeast culture), followed by the addition of 400 μL methanol with vigorous vortex to mix. The supernatant was transferred to new tubes. Repeat the extraction of the pellets by adding an additional 400 μL ethyl acetate. The supernatants were combined and dried in the vacufuge (Eppendorf). *Extraction Method B*: To extract total sterols (including sterol esters and free sterols) from yeast, 100 μL 60% (w/v) KOH and 100 μL ethanol was added to the cell pellets, then incubated at 86 °C for 1 hour for saponification. The mixture was then cooled down to room temperature and 400 μL petroleum ether was added followed by vortexing for 5 minutes. Organic phases were collected to new tubes. 400 μL ethyl acetate was added to the remaining aquatic phase and repeat the vortex step. Organic phases were combined and dried in vacufuge. The dried samples were dissolved in 40 μL methanol and analyzed using LC-MS. Samples extracted by *Extraction Method A* has higher recover ratio than that of *Extraction Method B*.

The samples were then analyzed by reverse phase LC-MS on a Shimadzu 2020 single quadrupole LC-MS (Poroshell 120, EC-C18, 3.0 × 100 mm, 2.7 μm) using positive ionization. To analyze sterols, the metabolites were separated under the linear gradient started from 80% methanol (v/v in water, 0.1% formic acid) to 100% methanol (v/v in water, 0.1% formic acid) for 8 min followed by 100% methanol (v/v in water, 0.1% formic acid) for 12 min at the flow rate of 0.5 ml/min. Data was acquired by the electrospray ionization mode. The sterols were analyzed using selected ion monitoring (SIM) with either the characteristic or possible mass-to-charge ratio (m/z^+) according to the structures and molecular weights. The quantities of campesterol were estimated by comparing to the standard curves using authentic campesterol standard solutions.

Analysis and quantification of progesterone and 5α-dihydroprogesterone in yeast

Progesterone and 5α-dihydroprogesterone were collected and analyzed from yeast pellets and medium. Extraction of yeast pellets: 100 μL acetone was added to yeast cell pellets (from 500 μL yeast culture), followed by the addition of 400 μL methanol with vigorous vortex to mix. The supernatant was transferred to new tubes. Repeat the extraction of the pellets by adding an additional 400 μL ethyl acetate. Extraction of medium: 400 μL of ethyl acetate was added to the culture medium, followed by vigorous vortex. The upper organic phase was collected and combined with pellet extracts, and dried in the vacufuge (Eppendorf). The samples were then analyzed by the same LC-MS setting as phytosterol analysis.

Genome sequencing

Genomic DNA was extracted with VWR Life Science Yeast Genomic DNA Purification Kit following the standard protocol from the vendor. The sequencing was done by Novogen Corporation. The chromatogram files generated by NGS platforms (like Illumina HiSeq TM 2000, MiSeq) are transformed by CASAVA Base Calling into sequencing reads, which are called Raw data or Raw reads. Both the sequenced reads and quality score information would be contained in FASTQ files. Raw data is filtered off the reads containing adapter and

low-quality reads to obtain clean data for subsequent analysis. The resequencing analysis is based on reads mapping to a common reference sequence (*S. cerevisiae* S288C) by BWA software. SAMTOOLS is used to detect SNP and InDel in functional genomics and get the mutation statistics.

Quantification of RNA expression level by quantitative RT-PCR

2 mL of 48-hour culture of yeast strains was cultivated as described in "Culture Conditions" section. Cell pellet was collected, and RNA was purified by Zymo YeaStar™ RNA kit. RNA concentration was quantified by Nanodrop (Molecular Device™). 200 ng of RNA of each strain was converted to cDNA by reverse transcription PCR kit from NEB. 1 μL of converted cDNA was used as the template and amplified by PCR using Taq polymerase (NEB). The constitutively expressed gene TDH3 was used as a control to normalize the cDNA concentration. PCR products were run electrophoresis and analyzed by ChemiDoc MP Imager (BIO RAD). The band intensity was quantified by the analysis tool of ChemiDoc MP Imager (BIO RAD). The intensity of target genes was normalized by the intensity of TDH3. Three independent replicates were examined in this experiment.

Application of CRISPR-Cas9 to inactive genes in yeast

The plasmids used for CRISPR-based gene inactivation in yeast (Fig. S8) were constructed through Gibson assembly of the backbone vector and DNA fragment encoding sgRNA and repair DNA (synthesized from IDT). The repair DNA contains 100 bp of homologous sequence of target cDNA incorporating an in-frame stop codon within ± 30 bp from the cutting site recognized by sgRNA (Figure S10A). The sgRNAs were designed using Benchling CRISPR tool (https://www.benchling.com/). The website provides on-target score (Doench, Fusi, et al, 2016) and off-target score (Hsu, et al, 2013) for the sgRNA, and sgRNAs with high scores in both on-target algorithm and specificity algorithm were selected for the gene inactivation. The sgRNA used to inactivate each gene were listed in Table S6. The sgRNA not targeting to any genes in yeast was used as a negative control (pYL1228, Table S2). The CRIPSPR/Cas9 design method was validated in a β-carotene-producing strain YYL23 (Table S1). The inactivation of the integrated gene *crtYB* in YYL23 can eliminate the synthesis of β-carotene and change the color of the strain from dark orange to white. The color change allowed the visualization of the inactivation of *crtYB*. The CRISPR/Cas9 designed by the method described above showed around 90% positive inactivation (Figure S10B).

Analysis and quantification of N-methylcanadine 1-hydroxy-N-methylcanadine in yeast

Canadine was fed to the yeast culture at inoculation with a final concentration of 12.5 μM. Culture was centrifuged to separate the liquid medium and the cell pellets, and the liquid medium was analyzed by LC-MS. The metabolites were separated under the linear gradient started from 20% methanol to 60% methanol (v/v in water, 0.1% formic acid) for 7 min at the flow rate of 0.5 ml/min. The quantities of canadine were estimated by comparing to the standard curves using authentic canadine standard solutions. The quantities of N-methylcanadine and 1-hydroxy-N-methylcanadine were estimated with mass intensity area multiplied by the ionization coefficient which calculated by using the principle of conservation of mass.

Supplementary Material

Refer to Web version on PubMed Central for supplementary material.

Acknowledgements

We thank Dr. Kaibiao Wang, Dr. Rongbin Hu, and Tiffany Chiu for valuable feedback and discussion in the preparation of the manuscript. This work was supported by the National Science Foundation (grant to Y.L., 1748695), Cancer Research Coordinating Committee Research Award (grant to Y.L., CRN-20-634571), and NIH New Innovator Award (grant to Y.L., DP2 AT011445-01).

Reference

(1). Dufourc EJ Sterols and membrane dynamics. J Chem Biol 2008, 1 (1-4), 63–77. DOI: 10.1007/s12154-008-0010-6. [PubMed: 19568799]

(2). Tong J; Manik MK; Im YJ Structural basis of sterol recognition and nonvesicular transport by lipid transfer proteins anchored at membrane contact sites. Proceedings of the National Academy of Sciences of the United States of America 2018, 115 (5), E856–E865. DOI: 10.1073/pnas.1719709115. [PubMed: 29339490]

(3). De Bruyne L; Hofte M; De Vleesschauwer D Connecting growth and defense: the emerging roles of brassinosteroids and gibberellins in plant innate immunity. Molecular plant 2014, 7 (6), 943–959. DOI: 10.1093/mp/ssu050. [PubMed: 24777987]

(4). Grouleff J; Irudayam SJ; Skeby KK; Schiott B The influence of cholesterol on membrane protein structure, function, and dynamics studied by molecular dynamics simulations. Biochim Biophys Acta 2015, 1848 (9), 1783–1795. DOI: 10.1016/j.bbamem.2015.03.029. [PubMed: 25839353]

(5). Hirz M; Richter G; Leitner E; Wriessnegger T; Pichler H A novel cholesterol-producing Pichia pastoris strain is an ideal host for functional expression of human Na,K-ATPase alpha 3 beta 1 isoform. Appl Microbiol Biot 2013, 97 (21), 9465–9478. DOI: 10.1007/s00253-013-5156-7.

(6). Zauber H; Burgos A; Garapati P; Schulze WX Plasma membrane lipid-protein interactions affect signaling processes in sterol-biosynthesis mutants in Arabidopsis thaliana. Frontiers in plant science 2014, 5, 78. DOI: 10.3389/fpls.2014.00078. [PubMed: 24672530]

(7). Luschnig C; Vert G The dynamics of plant plasma membrane proteins: PINs and beyond. Development 2014, 141 (15), 2924–2938. DOI: 10.1242/dev.103424. [PubMed: 25053426] Hrycay EG; Bandiera SM. The monooxygenase, peroxidase, and peroxygenase properties of cytochrome P450. Arch Biochem Biophys 2012, 522 (2), 71–89. DOI: 10.1016/j.abb.2012.01.003. [PubMed: 22266245]

(8). Simons K; Sampaio JL Membrane organization and lipid rafts. Cold Spring Harb Perspect Biol 2011, 3 (10), a004697. DOI: 10.1101/cshperspect.a004697 [PubMed: 21628426]

(9). Schaller H. The role of sterols in plant growth and development. Progress in lipid research 2003, 42 (3), 163–175. [PubMed: 12689617]

(10). Xu S; Chen C; Li Y Engineering of Phytosterol-Producing Yeast Platforms for Functional Reconstitution of Downstream Biosynthetic Pathways. ACS Synth Biol 2020, 9 (11), 3157–3170. DOI: 10.1021/acssynbio.0c00417. [PubMed: 33085451]

(11). Zweytick D; Leitner E; Kohlwein SD; Yu C; Rothblatt J; Daum G Contribution of Are1p and Are2p to steryl ester synthesis in the yeast Saccharomyces cerevisiae. Eur J Biochem 2000, 267 (4), 1075–1082. [PubMed: 10672016]

(12). Jacquier N; Schneiter R Mechanisms of sterol uptake and transport in yeast. The Journal of steroid biochemistry and molecular biology 2012, 129 (1-2), 70–78. DOI: 10.1016/j.jsbmb.2010.11.014. [PubMed: 21145395]

(13). DeLoache WC; Russ ZN; Dueber JE Towards repurposing the yeast peroxisome for compartmentalizing heterologous metabolic pathways. Nat Commun 2016, 7, 11152. DOI: 10.1038/ncomms11152. [PubMed: 27025684]

(14). Gao C; Cai Y; Wang Y; Kang BH; Aniento F; Robinson DG; Jiang L Retention mechanisms for ER and Golgi membrane proteins. Trends in plant science 2014, 19 (8), 508–515. DOI: 10.1016/j.tplants.2014.04.004. [PubMed: 24794130]

(15). Zhu J; Zhang ZT; Tang SW; Zhao BS; Li H; Song JZ; Li D; Xie Z A Validated Set of Fluorescent-Protein-Based Markers for Major Organelles in Yeast (Saccharomyces cerevisiae). mBio 2019, 10 (5). DOI: 10.1128/mBio.01691-19.

(16). Chen Q; Steinhauer L; Hammerlindl J; Keller W; Zou J Biosynthesis of phytosterol esters: identification of a sterol o-acyltransferase in Arabidopsis. Plant physiology 2007, 145 (3), 974–984. DOI: 10.1104/pp.107.106278. [PubMed: 17885082]

(17). Fischer MJ; Meyer S; Claudel P; Bergdoll M; Karst F Metabolic engineering of monoterpene synthesis in yeast. Biotechnology and bioengineering 2011, 108 (8), 1883–1892. DOI: 10.1002/bit.23129. [PubMed: 21391209]

(18). Ignea C; Trikka FA; Nikolaidis AK; Georgantea P; Ioannou E; Loupassaki S; Kefalas P; Kanellis AK; Roussis V; Makris AM; et al. Efficient diterpene production in yeast by engineering Erg20p into a geranylgeranyl diphosphate synthase. Metab Eng 2015, 27, 65–75. DOI: 10.1016/j.ymben.2014.10.008. [PubMed: 25446975]

(19). Rubat S; Varas I; Sepulveda R; Almonacid D; Gonzalez-Nilo F; Agosin E Increasing the intracellular isoprenoid pool in Saccharomyces cerevisiae by structural fine-tuning of a bifunctional farnesyl diphosphate synthase. Fems Yeast Res 2017, 17 (4). DOI: 10.1093/femsyr/fox032.

(20). Ding J; Huang X; Zhang L; Zhao N; Yang D; Zhang K Tolerance and stress response to ethanol in the yeast Saccharomyces cerevisiae. Appl Microbiol Biotechnol 2009, 85 (2), 253–263. DOI: 10.1007/s00253-009-2223-1. [PubMed: 19756577]

(21). Michelitsch MD; Weissman JS A census of glutamine/asparagine-rich regions: implications for their conserved function and the prediction of novel prions. Proceedings of the National Academy of Sciences of the United States of America 2000, 97 (22), 11910–11915. DOI: 10.1073/pnas.97.22.11910. [PubMed: 11050225]

(22). Stewart T; Wolfe BE; Fuchs SM Defining the role of the polyasparagine repeat domain of the S. cerevisiae transcription factor Azf1p. PloS one 2021, 16 (5), e0247285. DOI:10.1371/journal.pone.0247285. [PubMed: 34019539]

(23). Escobar-Henriques M; Daignan-Fornier B Transcriptional regulation of the yeast gmp synthesis pathway by its end products. The Journal of biological chemistry 2001, 276 (2), 1523–1530. DOI: 10.1074/jbc.M007926200. [PubMed: 11035032]

(24). Zhang M; Bennett D; Erdman SE Maintenance of mating cell integrity requires the adhesin Fig2p. Eukaryot Cell 2002, 1 (5), 811–822. DOI: 10.1128/EC.1.5.811-822.2002. [PubMed: 12455698]

(25). Alberti S; Gitler AD; Lindquist S A suite of Gateway cloning vectors for high-throughput genetic analysis in Saccharomyces cerevisiae. Yeast 2007, 24 (10), 913–919. DOI: 10.1002/yea.1502. [PubMed: 17583893]

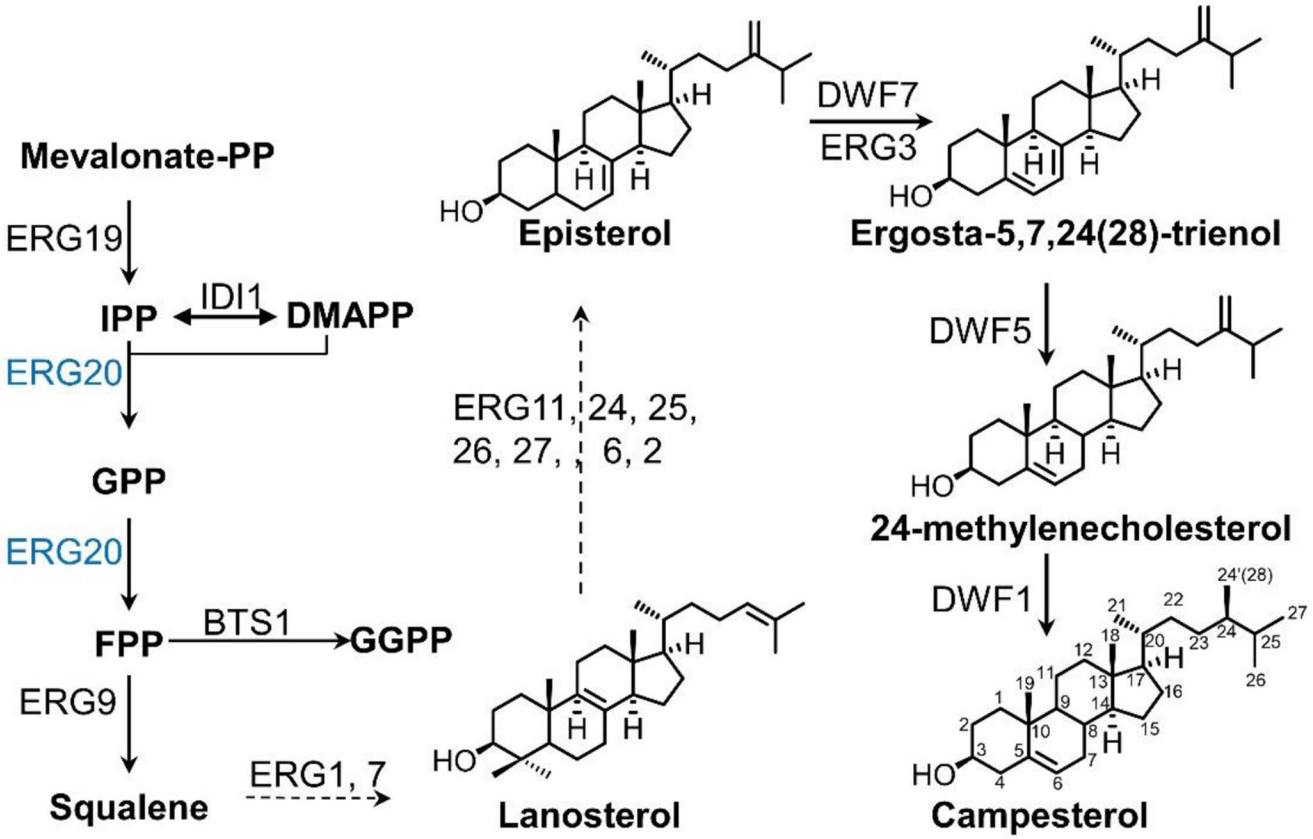

Figure 1.

The putative biosynthetic pathway of campesterol in engineered yeaststrains. The dashed arrows represent multiple steps. ERG3 and DWF5 having the same function: Δ7-sterol-C5(6)-desaturase 1; DWF7: Δ^{7}-sterol-C5(6)-desaturase 1; DWF5: C7(8)-reductase; DWF1: $\Delta^{24(28)}$-sterol reductase.

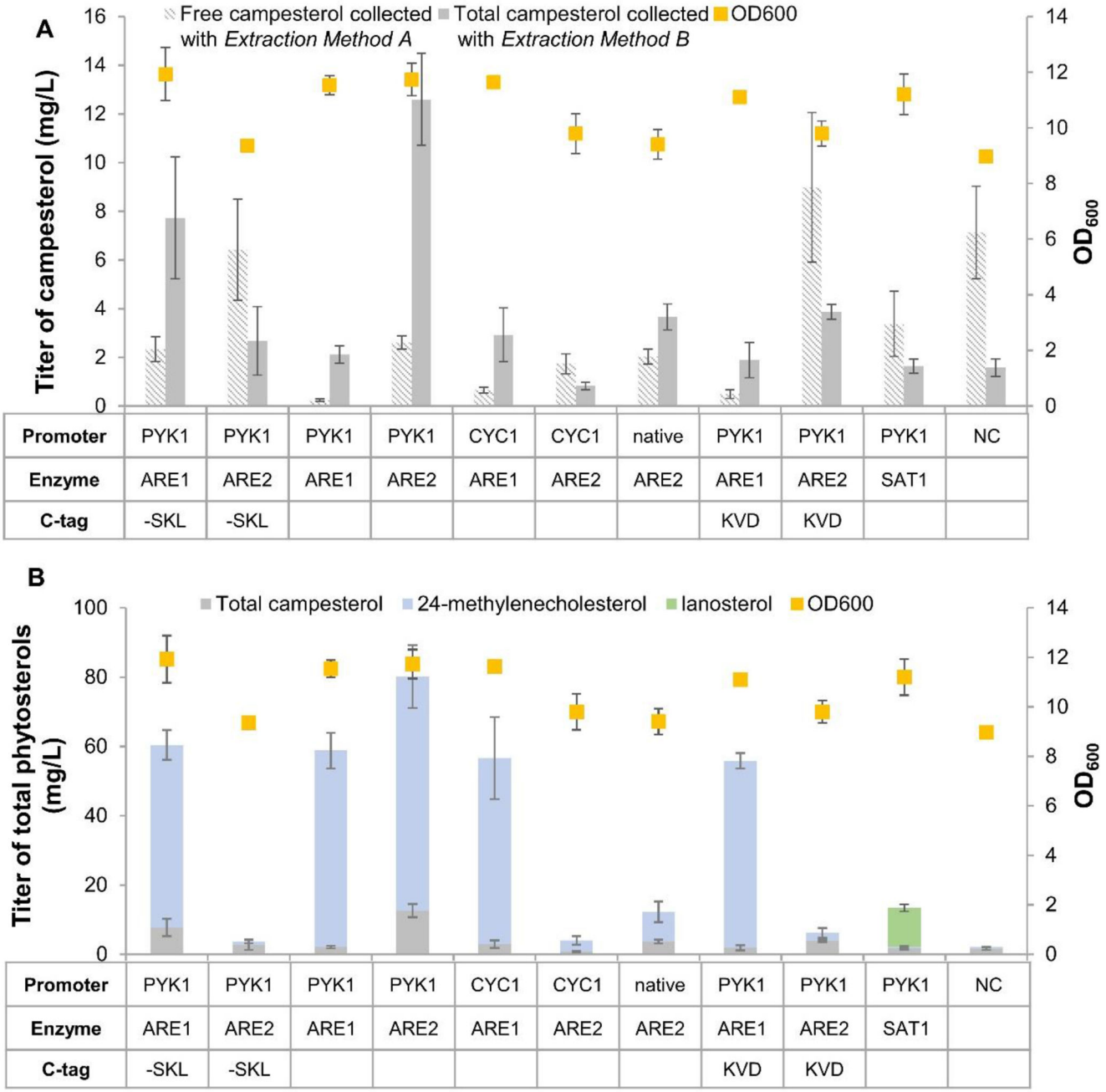

Figure 2.

The effects of ARE1 and ARE2 to sterol production in YYL67. **(A)** Campesterol production of YYL67 expressing ARE1 or ARE2 using different promoters and/or with different C-terminal localization tags. **(B)** Production of total phytosterols in YYL67 expressing ARE1 or ARE2 using different promoters and/or with different C-terminal localization tags. YYL67 harboring an empty vector was used as a negative control, NC. Free campesterol was extracted without saponification using *Extraction Method A*. Total campesterol was extracted by saponification using KOH, as described in *Extraction Method B. Extraction*

Method B exhibits more significant sample loss than *Extraction Method A* due to the harsh treatment of the sample during saponification. Error bars represent standard deviation of three biological replicates.

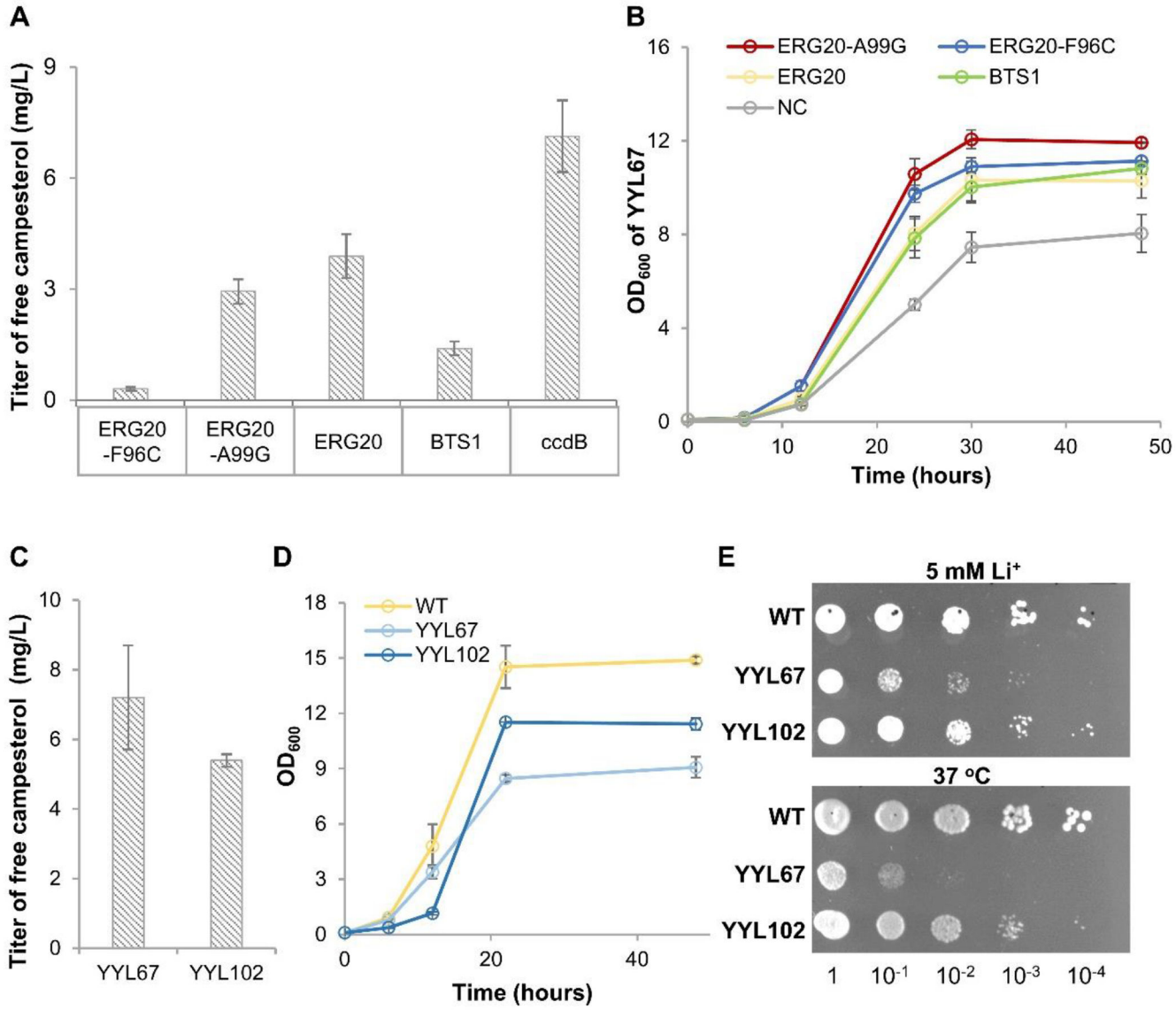

Figure 3.

Effects of ERG20 mutants on campesterol production in YYL67. (A) Production of campesterol in YYL67 expressing ERG20, ERG20^{F96C}, ERG20^{A99G}, and BTS1. The yeast strain harboring an empty vector was used as a negative control, NC. (B) Growth of YYL67 expressing ERG20, ERG20^{F96C}, ERG20^{A99G}, and BTS1 when cultured in SDM with auxotrophic selections at 30 °C. (C) Production of campesterol in the optimized strain YYL102 (YYL67 expressing ERG20^{A99G} and ARE2 through genomic integration, Table S1), YYL67. (D) Growth of wild-type (WT) yeast, YYL67, and YYL102 when cultured in SDM at 30 °C. (E) Li+ tolerance and heat tolerance of YYL67 and YYL102. Error bars represent standard deviation of three biological replicates.

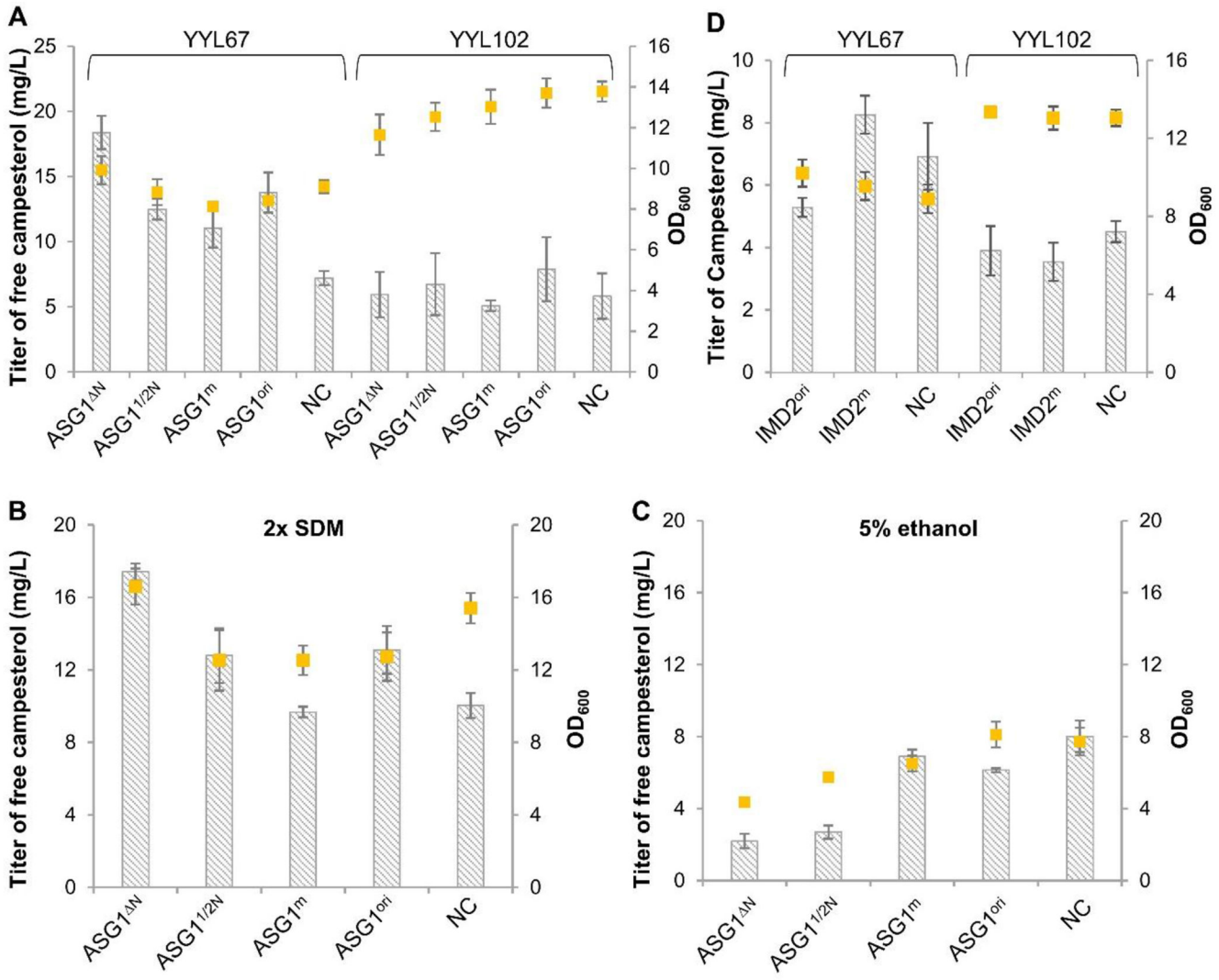

Figure 4.

Effects of ASG1 mutants on sterol production and yeast growth in YYL67 and YYL102. (A) Production of campesterol and stationary OD_{600} of YYL67 or YYL102 expressing different ASG1 variants ($ASG1^{\Delta N}$, $ASG1^{1/2N}$, $ASG1^{m}$, and $ASG1^{ori}$) cultured in SDM. (B) Production of campesterol and stationary OD_{600} of the YYL67 expressing different ASG1 variants ($ASG1^{\Delta N}$, $ASG1^{1/2N}$, $ASG1^{m}$, and $ASG1^{ori}$) when cultured in the 2× SDM. (C) Production of campesterol and stationary OD_{600} of YYL67 expressing different ASG1 variants ($ASG1^{\Delta N}$, $ASG1^{1/2N}$, $ASG1^{m}$, and $ASG1^{ori}$) when cultured in SDM supplement with 5% ethanol. (D) Production of campesterol and stationary OD_{600} of YYL67 or YYL102 expressing $IMD2^{m}$ or $IMD2^{ori}$. The yeast strain harboring an empty vector was used as a negative control, NC. Error bars represent standard deviation of three biological replicates.

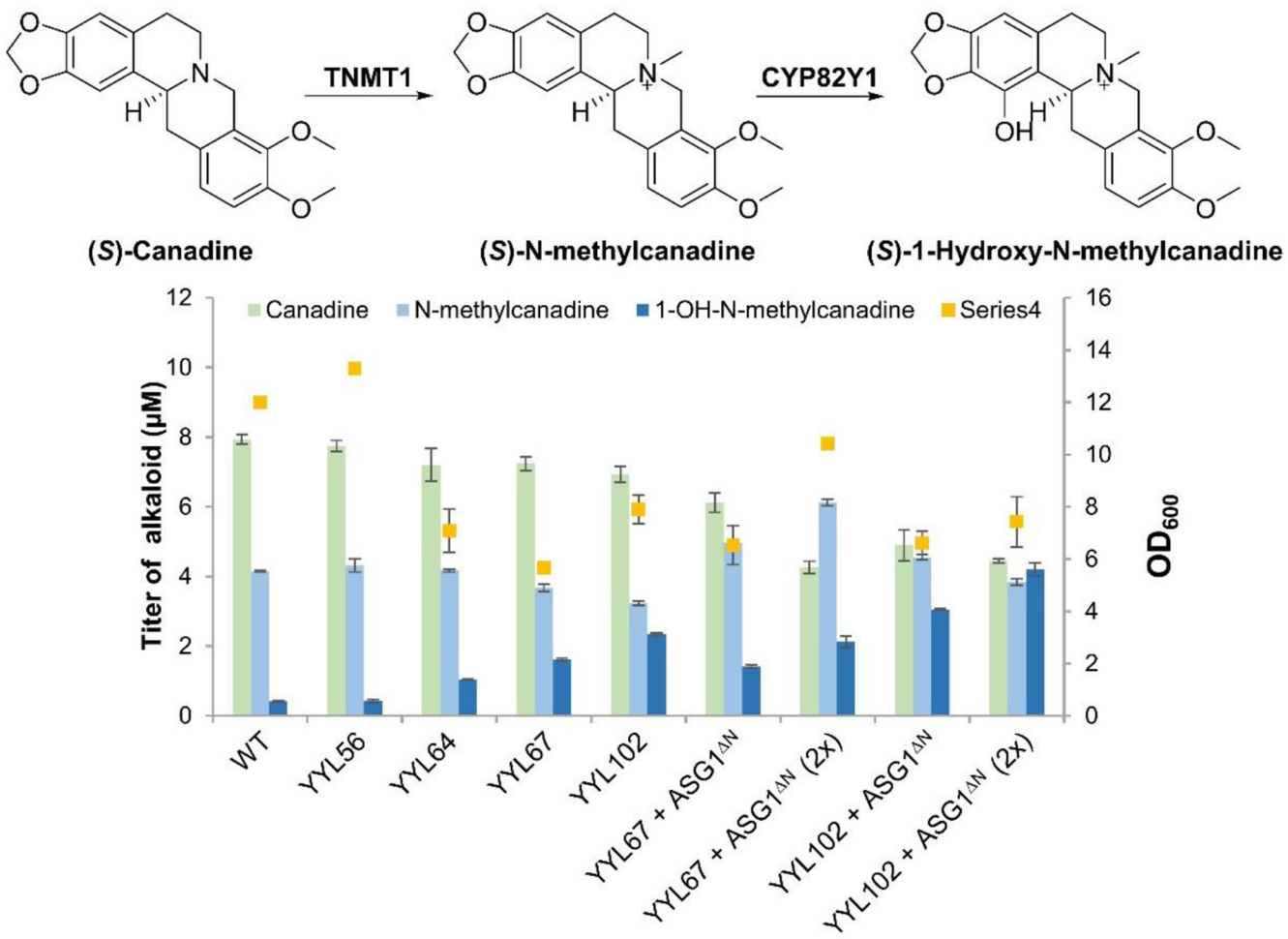

Figure 5.

Activity of the plant cytochrome P450 CYP82Y1 towards the synthesis of 1-hydroxy-N-methylcanadine in different yeast. The biosynthetic pathway from canadine to 1-hydroxy-N-methylcanadine catalyzed by TNMT and CYP82Y1 is illustrated on the top. Production of 1-hydroxy-N-methylcanadine of different yeast strains expressing TNMT1 and CYP82Y1: wile type (WT) yeast strain, YYL56, YYL64, YYL67, YYL102, YYL67 expressing $ASG1^{\Delta N}$, YYL102 expressing $ASG1^{\Delta N}$, cultured in either standard SDM or 2× SDM (marked as ″2×″). Error bars represent standard deviation of three biological replicates.